Ae4 (Slc4a9) is an electroneutral monovalent cation-dependent Cl^-/HCO_3^- exchanger

Gaspar Peña-Münzenmayer,[1] Alvin T. George,[1] Gary E. Shull,[2] James E. Melvin,[1] and Marcelo A. Catalán[1]

[1]Secretory Mechanisms and Dysfunction Section, National Institute of Dental and Craniofacial Research, National Institutes of Health, Bethesda, MD 20892

[2]Department of Molecular Genetics, Biochemistry, and Microbiology, University of Cincinnati College of Medicine, Cincinnati, OH 45267

Ae4 (Slc4a9) belongs to the Slc4a family of Cl^-/HCO_3^- exchangers and Na^+-HCO_3^- cotransporters, but its ion transport cycle is poorly understood. In this study, we find that native Ae4 activity in mouse salivary gland acinar cells supports Na^+-dependent Cl^-/HCO_3^- exchange that is comparable with that obtained upon heterologous expression of mouse Ae4 and human AE4 in CHO-K1 cells. Additionally, whole cell recordings and ion concentration measurements demonstrate that Na^+ is transported by Ae4 in the same direction as HCO_3^- (and opposite to that of Cl^-) and that ion transport is not associated with changes in membrane potential. We also find that Ae4 can mediate Na^+-HCO_3^- cotransport–like activity under Cl^--free conditions. However, whole cell recordings show that this apparent Na^+-HCO_3^- cotransport activity is in fact electroneutral HCO_3^-/Na^+-HCO_3^- exchange. Although the Ae4 anion exchanger is thought to regulate intracellular Cl^- concentration in exocrine gland acinar cells, our thermodynamic calculations predict that the intracellular Na^+, Cl^-, and HCO_3^- concentrations required for Ae4-mediated Cl^- influx differ markedly from those reported for acinar secretory cells at rest or under sustained stimulation. Given that K^+ ions share many properties with Na^+ ions and reach intracellular concentrations of 140–150 mM (essentially the same as extracellular [Na^+]), we hypothesize that Ae4 could mediate K^+-dependent Cl^-/HCO_3^- exchange. Indeed, we find that Ae4 mediates Cl^-/HCO_3^- exchange activity in the presence of K^+ as well as Cs^+, Li^+, and Rb^+. In summary, our results strongly suggest that Ae4 is an electroneutral Cl^-/nonselective cation–HCO_3^- exchanger. We postulate that the physiological role of Ae4 in secretory cells is to promote Cl^- influx in exchange for K^+(Na^+) and HCO_3^- ions.

INTRODUCTION

Bicarbonate (HCO_3^-) transporters play important roles in many physiological processes such as intracellular pH (pH_i) regulation (Russell and Boron, 1976), acid–base transport (Gawenis et al., 2007), and Cl^- (Leviel et al., 2010) and HCO_3^- secretion (Ishiguro et al., 1996), as well as epithelial fluid secretion (Walker et al., 2002). *SLC4-like* genes encode for a family of HCO_3^--transporting proteins in bacteria, plants, and animals (Parker and Boron, 2013). The 10 mammalian SLC4 members (SLC4A1–5 and SLC4A7–11) mediate diverse HCO_3^--transporting activities, including Cl^-/HCO_3^- exchange, Na^+-HCO_3^- cotransport, and Na^+-driven Cl^-/HCO_3^- exchange. It is well accepted that SLC4A1–3 (AE1–3, respectively) are Na^+-independent Cl^-/HCO_3^- exchangers, whereas SLC4A4, -5, and -7 (NBCe1, NBCe2, and NBCn1, respectively) are Na^+-HCO_3^- cotransporters (Parker and Boron, 2013; Romero et al., 2013). Conversely, the functional properties of SLC4A8–11 have not been as well defined, but it appears that they may act as either Na^+-independent (SLC4A9/AE4; Tsuganezawa et al., 2001; Ko et al., 2002) or Na^+-driven Cl^-/HCO_3^- exchangers (SLC4A8, -9, and -10; Wang et al., 2000; Leviel et al., 2010; Peña-Münzenmayer et al., 2015), as well as Na^+-HCO_3^- cotransporters (SLC4A8, -9, and -10; Grichtchenko et al., 2001; Wang et al., 2001; Parker et al., 2008; Chambrey et al., 2013). In contrast, it has been suggested that SLC4A11 (BTR1) serves as a borate transporter (Park et al., 2004), Na^+-dependent OH^- transporter (Ogando et al., 2013), NH_3/H^+ cotransporter (Zhang et al., 2015), or DIDS-stimulated H^+ (OH^-) transporter (Kao et al., 2015).

The current evidence suggests that SLC4 family members play an important role in exocrine gland fluid secretion by promoting intracellular Cl^- accumulation in secretory acinar cells (Nguyen et al., 2004; Melvin et al., 2005). Indeed, we recently found that Ae2 (Slc4a2) and Ae4 (Slc4a9) are functionally expressed in salivary gland acinar cells, but only Ae4 appears to play an important role in fluid secretion (Peña-Münzenmayer et al., 2015). There is no agreement regarding the Ae4 ion–transporting mechanism, but it has been suggested that Ae4 may

Correspondence to Marcelo A. Catalán: marcelo.catalan@nih.gov

Abbreviations used in this paper: pH_i, intracellular pH; SMG, submandibular gland.

The Rockefeller University Press $30.00
J. Gen. Physiol. 2016 Vol. 147 No. 5 423–436
www.jgp.org/cgi/doi/10.1085/jgp.201611571

be a Na^+-independent Cl^-/HCO_3^- exchanger (Tsuganezawa et al., 2001; Ko et al., 2002) or a Na^+-HCO_3^- cotransporter (Chambrey et al., 2013). In contrast, we found that Ae4 acts as a Na^+-dependent Cl^-/HCO_3^- exchanger (Peña-Münzenmayer et al., 2015) in salivary gland acinar cells, but the nature of the Na^+ dependency is unknown.

The main goal of this study was to gain insight into the Na^+ dependence of the ion-transporting mechanism used by Ae4, which may provide a better understanding of how Ae4 supports fluid secretion by the exocrine salivary glands. Mouse Ae4 (Slc4a9)-mediated transport was associated with HCO_3^-, Cl^-, Na^+, and K^+ fluxes, with no change in membrane potential, revealing that Ae4 is an electroneutral, nonselective cation-dependent Cl^-/HCO_3^- exchanger. We propose that the lower intracellular [Cl^-] observed in the salivary gland secretory cells of *Ae4*$^{-/-}$ mice is the consequence of the loss of Ae4-mediated intracellular Cl^- accumulation in exchange for $KHCO_3$ efflux.

MATERIALS AND METHODS

Animals

Mice were housed in micro-isolator cages with ad libitum access to laboratory chow and water with a 12-h light/dark cycle. Experiments were performed on 2–4-mo-old female and male animals. All animal procedures were approved by the National Institute of Dental and Craniofacial Research, National Institutes of Health, Animal Care and Use Committee (ASP 13-686). Acinar-specific *Ae2*$^{-/-}$ mice were generated by crossing conditional knockout *Ae2* mice (*Ae2*$^{flox/flox}$; Coury et al., 2013) with knock-in mice expressing Cre recombinase under the Aqp5 promoter (ACID mice; Flodby et al., 2010) as previously described (Peña-Münzenmayer et al., 2015). Mice lacking Ae2 and Ae4 in salivary gland acinar cells (*Ae2*$^{-/-}$-*Ae4*$^{-/-}$ mice) were obtained by making the proper crosses between *Ae2*$^{flox/flox}$, ACID, and *Ae4*$^{-/-}$ (Simpson et al., 2007) mice.

Plasmids

Plasmids encoding *Mus musculus* Ae4 (Slc4a9) transcript variant 3 (GenBank accession no. NM_172830) and *Homo sapiens* AE4 (SLC4A9) transcript variant 2 (GenBank accession no. NM_031467) were obtained from OriGene.

Mouse submandibular gland (SMG) acinar cell isolation

Mice were euthanized by CO_2 asphyxiation followed by cervical dislocation. SMGs from *Ae2*$^{-/-}$ and *Ae2*$^{-/-}$-*Ae4*$^{-/-}$ mice were surgically removed and finely minced with scissors and then digested by two consecutive incubation steps of 25 min each with 0.5 mg/ml collagenase 2 (type 2; Worthington Biochemical Corporation) in basal medium eagle (BME; Sigma-Aldrich). All solutions were gassed continuously with 95% O_2/5% CO_2 and maintained at 37°C.

Cell culture and transfections

CHO-K1 cells (Sigma-Aldrich) were grown in Petri dishes containing F12 medium (Invitrogen) supplemented with 10% (vol/vol) fetal bovine serum (Invitrogen) and penicillin-streptomycin-glutamine (100 U/ml, 100 µg/ml, 292 µg/ml) and maintained in a humidified 5% CO_2/95% air atmosphere. Cells were electroporated (Nucleofector II; Amaxa) with the plasmids mentioned above (4 µg DNA per reaction) using the Nucleofector kit V (Lonza) according to the manufacturer's instructions and seeded onto 5-mm-diameter coverslips (Warner Instruments). It is important to note that at least 4 µg DNA was required per electroporation to measure a robust Ae4 activity in CHO-K1 cells 18–20 h after electroporation.

pH_i, [Cl^-], [Na^+], and [K^+] measurements

The fluorescent ion-sensitive dyes BCECF-AM (2′,7′-bis-(2-carboxyethyl)-5-(and-6)-carboxyfluorescein, acetoxymethyl ester; Rink et al., 1982), SPQ (6-methoxy-*N*-[3-sulfopropyl] quinolinium; Illsley and Verkman, 1987), SBFI-AM (1,3-benzenedicarboxylic acid, 4,4′-[1,4,10-trioxa-7,13-diazacyclopentadecane-7,13-diylbis(5-methoxy-6,12-benzofurandiyl)]bis-, tetrakis[(acetyloxy)methyl] ester), and PBFI-AM (1,3-benzenedicarboxylic acid, 4,4′-[1,4,10,13-tetraoxa-7,16-diazacyclooctadecane-7,16-diylbis(5-methoxy-6,2-benzofurandiyl)]bis-, tetrakis[(acetyloxy)methyl] ester; Minta and Tsien, 1989) were purchased from Invitrogen and used to measure pH_i, [Cl^-], [Na^+], and [K^+], respectively. CHO-K1 cells were loaded with the different ion-sensitive dyes as follows: 2 µM BCECF-AM for 15 min at 37°C (95% O_2/5% CO_2), 10 µM SBFI-AM or 10 µM PBFI-AM for 1.5 h at room temperature (95% O_2/5% CO_2). For intracellular [Cl^-] measurements, CHO-K1 cells were exposed to a hypotonic loading solution containing 10 mM SPQ as previously described (Chao et al., 1989). Dispersed acinar cells from SMGs were loaded with 2 µM BCECF-AM (15 min at 37°C and continuously gassed with 95% O_2/5% CO_2).

Imaging experiments were performed using an inverted microscope (IX71; Olympus) equipped with a Polychrome IV Imaging System coupled to a high-speed digital camera (Till Photonics). Images were acquired by alternate excitation at 490 and 440 nm (BCECF), 340 and 380 nm (SBFI and PBFI), or 340 nm (SPQ). Emissions were captured at 530 nm (BCECF) or 510 nm (SPQ, SBFI and PBFI) using Imaging WorkBench 6.0 software (INDEC BioSystems). The temperature of the solutions (listed in Table 1) was kept at 37°C during the experiments using a CL-100 bipolar temperature controller (Warner Instruments).

Simultaneous electrophysiological and imaging experiments

Simultaneous whole cell recordings (voltage and current clamp modes) and intracellular [Cl^-] or pH_i mea-

Table 1. **Solutions used in imaging experiments**

Component	Solution name										
	A	**B**	**C**	**D**	**E**	**F**	**G**	**H**	**I**	**J**	**K**
	mM	*mM*	*mM*	*mM*	*mM*	*mM*	*mM*	*mM*	*mM*	*mM*	*mM*
Na^+	145	145			145	145	145	145			
K^+	4.3	4.3	4.3	4.3	4.3	4.3	4.3	4.3	4.3	145	145
NMDG			120	120					120		
Ca^{2+}	1	1	1	1	1	1	1	1	1	1	1
Mg^{2+}	1	1	1	1	1	1	1	1	1	1	1
Choline			25	25					25		
Cl^-	128.3	4	128.3	4	153.3	4				124	4
HCO_3^-	25	25	25	25				25	25	25	25
Gluconate		124.3				149.3	8.3	8.3	8.3		120
Glutamate				124.3			145	120	120		
Glucose	5	5	5	5	5	5	5	5	5	5	5
HEPES	10	10	10	10	10	10	10	10	10	10	10

The pH value for all solutions was 7.4.

surements were performed at room temperature (22°C) on CHO-K1 cells using an Axopatch 200B amplifier (Molecular Devices) and a Polychrome IV monochromator (Till Photonics). The membrane voltage and the macroscopic currents were acquired to a computer hard drive using Clampex 10 software (Molecular Devices) via a Digidata 1440 Interface (Molecular Devices). BCECF- and SPQ-associated fluorescent images were acquired as described in the previous section using pipette (intracellular) solutions supplemented with 100 µM BCECF (free acid) or 1 mM SPQ, respectively. Membrane potential measurements were corrected by the changes in liquid junction potential (Barry, 1994).

Glass pipettes (Warner Instruments) were pulled using a P97 puller (Sutter Instrument) to give a resistance of 2–3 MΩ using the solutions listed in Table 2. The seal resistance was continuously calculated according to Ohm's law from the difference in the membrane potential in response to −30-pA (current clamp mode), 60-mV (voltage clamp experiments at −100 mV), or −20-mV (voltage clamp experiments at 0 mV) square pulses of 250 ms every 5 s. Experiments in which the seal resistance was >500 MΩ throughout the experiment were considered for analysis.

Experimental solutions

The composition of external solutions used for single pH_i, Cl^-, Na^+, and K^+ measurements are given in Table 1. The composition of pipette (internal) and external solutions used in simultaneous whole cell recordings and intracellular Cl^- or pH measurements are given in Table 2. The composition of the external solutions used to evaluate the selectivity of Ae4 for inorganic monovalent cations is shown in Table 3.

The osmolality of the external and pipette solutions were measured by a freezing-point depression osmometer (Advanced Instruments) and adjusted to 300 mOsm/kg with sucrose. All of the reagents used for the solutions were from Sigma-Aldrich unless otherwise indicated.

ΔG calculations

The changes in free Gibbs energy associated with the Ae4-mediated transport were calculated (at 37°C) using the following formula:

Table 2. **Solutions used in combined electrophysiological and fluorescence measurements**

Component	Solution name							
	L	**M**	**N**	**O**	**P**	**Q**	**R**	**S**
	mM	*mM*	*mM*	*mM*	*mM*	*mM*	*mM*	*mM*
Na^+			100				140	140
$NMDG^+$	100	100		140	140	125		
Ca^{2+}		1	1				1	1
Mg^{2+}	1	1	1	2	2	2	1	1
Choline	25	25	25			15		
Cl^-	42	4	4	15	4	4	4	4
HCO_3^-	25	25	25			15		25
Glutamate	60	100	100	129	140	125	140	115
EGTA	10			1	1	1		
Tris	10			1	1	1		
Glucose		5	5				5	5
HEPES	10	10	10	1	1	1	10	10

The pH value for solutions L–N, R, and S was 7.4. The pH value for solutions O–Q was 7.2.

Table 3. **Solutions used in cation selectivity experiments**

Component	Solution name														
	Na^+ 5	Na^+ 25	Na^+ 50	Na^+ 100	Na^+ 125	Na^+ 150	K^+ 5	K^+ 25	K^+ 50	K^+ 100	K^+ 125	K^+ 150	Li^+ 100	Rb^+ 100	Cs^+ 100
	mM	*mM*	*mM*	*mM*	*mM*	*mM*	*mM*	*mM*	*mM*	*mM*	*mM*	*mM*	*mM*	*mM*	*mM*
Na^+	5	25	50	100	125	150									
K^+							5	25	50	100	125	150			
Li^+													100		
Rb^+														100	
Cs^+															100
$NMDG^+$	120	125	100	50	25		120	125	100	50	25		25	25	25
Ca^{2+}	1	1	1	1	1	1	1	1	1	1	1	1	1	1	1
Mg^{2+}	1	1	1	1	1	1	1	1	1	1	1	1	1	1	1
Choline	25						25						25	25	25
Cl^-	4	4	4	4	4	4	4	4	4	4	4	4	4	4	4
HCO_3^-	25	25	25	25	25	25	25	25	25	25	25	25	25	25	25
Glutamate	125	125	125	125	125	125	125	125	125	125	125	125	125	125	125
Glucose	5	5	5	5	5	5	5	5	5	5	5	5	5	5	5
HEPES	10	10	10	10	10	10	10	10	10	10	10	10	10	10	10

The pH value for all solutions was 7.4.

$$\Delta G = RT\left[\ln\left(\frac{Cl^-_o}{Cl^-_i}\right) + 2*\ln\left(\frac{HCO_3^-_i}{HCO_3^-_o}\right) + \ln\left(\frac{Na^+_i}{Na^+_o}\right)\right] \quad (1)$$

$$\Delta G = RT\left[\ln\left(\frac{Cl^-_o}{Cl^-_i}\right) + 3*\ln\left(\frac{HCO_3^-_i}{HCO_3^-_o}\right) + 2*\ln\left(\frac{Na^+_i}{Na^+_o}\right)\right] \quad (2)$$

$$\Delta G = RT\left[2*\ln\left(\frac{Cl^-_o}{Cl^-_i}\right) + 3*\ln\left(\frac{HCO_3^-_i}{HCO_3^-_o}\right) + \ln\left(\frac{Na^+_i}{Na^+_o}\right)\right], \quad (3)$$

where R is the ideal gas constant $8.31*10^{-3}$ kJ*mol^{-1}*K^{-1}, T is the temperature in Kelvin (310.15 K = 37°C), and the other parameters are the intracellular and extracellular Cl^-, HCO_3^-, and Na^+ concentrations.

Ae4 dependence on Na^+ and K^+ concentrations

The dependence of Ae4 for Na^+ and K^+ ions was obtained by fitting the Ae4 activities measured at different $[Na^+]_o$ and $[K^+]_o$ to the following Hill function using Origin 8.0 software (OriginLab):

$$R_{Cation} = R_{Min} + \frac{(R_{Max} - R_{Min})*[\text{Cation}]^{nH}}{EC_{50}{}^{nH} + [\text{Cation}]^{nH}}, \quad (4)$$

where R_{Cation} is the alkalinization rate in response to a reduction in external $[Cl^-]$ at different [Cation] and R_{Min} and R_{Max} correspond to the minimal and maximal alkalinization rates. The EC_{50} is the concentration required to achieve 50% of the maximal effect, and nH is the Hill number.

Statistical analysis

Results are presented as the mean ± SEM. Statistical significance was determined using the Student's t test. Multiple-sample comparisons were performed using one-way ANOVA followed by Bonferroni's post hoc test. A p-value <0.05 was considered statistically significant. Origin 8.0 software was used for statistical calculations. All experiments were performed for each condition using preparations from three or more separate mice or cell electroporations.

RESULTS

Ae4 is an electroneutral, Na^+-dependent Cl^-/HCO_3^- exchanger

The Cl^-/HCO_3^- exchanger activity in mouse salivary gland acinar cells is dependent on the expression of the *Ae2* and *Ae4* genes (Peña-Münzenmayer et al., 2015). Consequently, the acinar cells from *Ae2*$^{-/-}$ mice serve as a physiological model to isolate native Ae4-mediated Cl^-/HCO_3^- exchanger activity. As seen in Fig. 1 A (black circles), an extensive intracellular alkalinization consistent with Cl^-/HCO_3^- exchange was observed when most of the extracellular Cl^- was isotonically replaced by gluconate (Cl^- concentration was reduced from 128.3 mM to 4 mM; see ion composition of solutions A and B in Table 1). The Cl^-/HCO_3^- exchange activity present in *Ae2*$^{-/-}$ acinar cells was dramatically reduced when external Na^+ was isotonically replaced with the large organic cation NMDG (Fig. 1 A, green circles), demonstrating that Ae4 activity is Na^+ dependent. Furthermore, there was nearly a total absence of an intracellular alkalinization in acinar cells from mice lacking Ae2 and Ae4 (*Ae2*$^{-/-}$-*Ae4*$^{-/-}$) in the presence of external Na^+, in agreement with Ae4 being the major anion exchanger present in acinar cells from *Ae2*$^{-/-}$ mice (Fig. 1 A, blue circles). A summary of the alkalinization rates calculated from experiments like those shown in Fig. 1 A (red lines) are presented in Fig. 1 B.

To further characterize the Na^+ dependence of Ae4, we measured its Cl^-/HCO_3^- exchanger activity by heterologous expression of mouse Ae4 cDNA in CHO-K1 cells. As seen in Fig. 2 A, an intracellular alkalinization comparable with that seen in native *Ae2*$^{-/-}$ acinar cells (Fig. 1) was observed in Ae4-transfected CHO-K1 cells (black circles) when most of the extracellular Cl^- was replaced by gluconate. Like *Ae2*$^{-/-}$ acinar cells, the Cl^-/HCO_3^- exchanger activity in Ae4-trans-

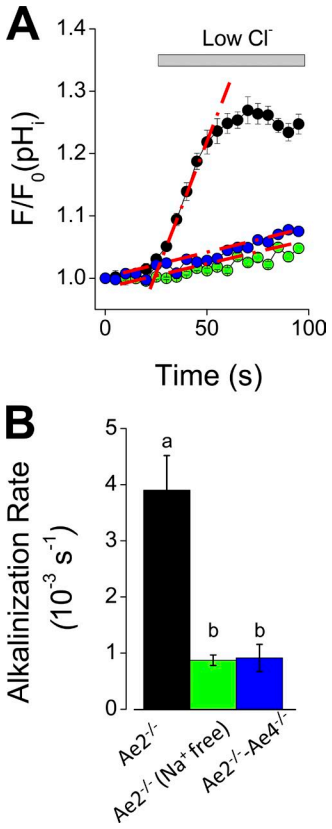

Figure 1. **Na^+ dependence of the Cl^-/HCO_3^- exchanger in SMG acinar cells from the *Ae2*$^{-/-}$ mouse.** (A) pH_i measurements performed on isolated acinar cells loaded with the pH indicator BCECF-AM. An intracellular alkalinization was observed in *Ae2*$^{-/-}$ cells in response to a reduction in $[Cl^-]_o$ in the presence of external Na^+ (black circles; $n = 8$; switching from solution A to B [Table 1]). In contrast, little, if any, alkalinization was observed in the absence of external Na^+ in *Ae2*$^{-/-}$ cells (green circles; $n = 7$; switching from solution C to D [Table 1]) or in *Ae2*$^{-/-}$-*Ae4*$^{-/-}$ cells using a Na^+-containing external solution (blue circles; $n = 8$; switching from solution A to B [Table 1]). Exchanger activity was calculated by linear regression analysis of the initial alkalinization response induced by a reduction in $[Cl^-]_i$ (discontinuous red lines). Results are presented as the mean ± SEM. (B) Summary of experiments as shown in A. Data are expressed as the mean ± SEM of at least five acinar cells per experiment from at least three cell preparations. For *Ae2*$^{-/-}$ mice, the black bar is significantly greater, "a" compared with "b" ($P < 0.05$, one-way ANOVA followed by Bonferroni's post hoc test).

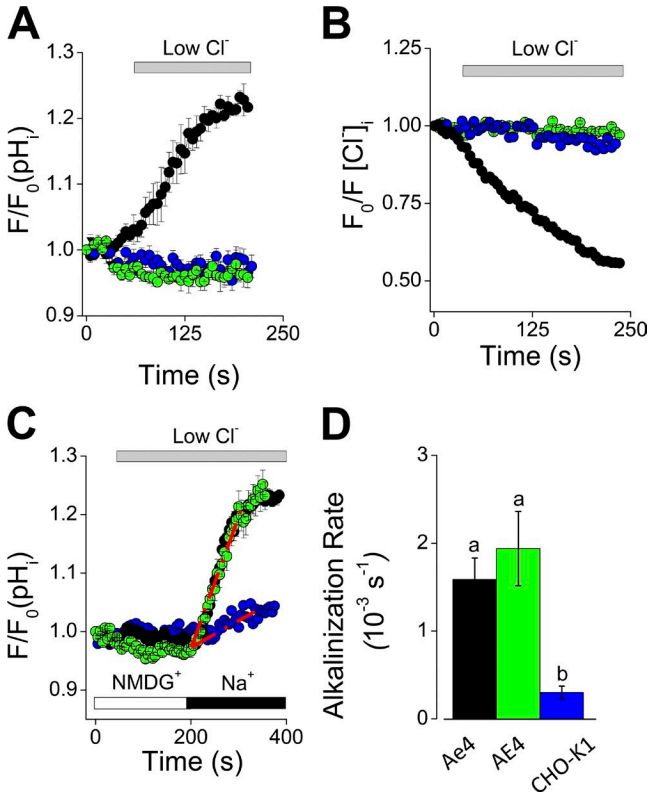

Figure 2. **Na^+ dependence of mouse Ae4 and human AE4 exchangers expressed in CHO-K1 cells.** (A) CHO-K1 cells transfected with a plasmid containing the mouse Ae4 cDNA were loaded with BCECF-AM. A rapid increase in pH_i was observed upon external Cl^- reduction in the presence of external Na^+ (black circles; $n = 11$; changing solution A to B [Table 1]). In contrast, the rise in pH_i was prevented when Na^+ (blue circles; $n = 6$; changing solution C to D [Table 1])- or HCO_3^- (green circles; $n = 8$; changing solution E to F [Table 1])-free external solutions were used. (B) Similar experiments as shown in A using the same external solutions performed on CHO-K1 cells expressing mouse Ae4 but using the Cl^- indicator SPQ. A rapid loss of intracellular $[Cl^-]$ was observed upon external $[Cl^-]$ reduction in the presence of external Na^+ (black circles; $n = 10$), but there was essentially no change in $[Cl^-]_i$ in HCO_3^- (green circles; $n = 7$)- or Na^+ (blue circles; $n = 6$)-free external solutions. (C) There was no change in pH_i in CHO-K1 cells expressing mouse Ae4 (black circles; $n = 8$) and human AE4 (green circles; $n = 5$) in response to a decrease in the external $[Cl^-]$ in a NMDG-containing solution (changing solution C to D [Table 1]), but there was a dramatic increase in the pH_i when switched to a Na^+-containing external solution. These manipulations resulted in little change in pH_i on nontransfected cells (blue circles; $n = 9$; changing solution D to B [Table 1]). (A–C) Results are presented as the mean ± SEM. (D) Summary of the experiments as shown in C. Data are expressed as the mean ± SEM of at least five cells per experiment from at the least three different electroporations. For nontransfected CHO-K1 cells, the blue bar is significantly less, "a" compared with "b" ($P < 0.05$, one-way ANOVA followed by Bonferroni's post hoc test).

fected cells was Na^+ dependent, as indicated by the lack of an intracellular alkalinization when external Na^+ was replaced by NMDG (Fig. 2 A, blue circles). Furthermore, the Na^+-dependent, Ae4-mediated alkalinization was absent under extracellular HCO_3^--free conditions (Fig. 2 A, green circles), consistent with Cl^-/HCO_3^- exchange.

We also evaluated the Na^+ dependence of Ae4-mediated Cl^- fluxes in CHO-K1 cells using the Cl^--sensitive dye SPQ. As shown in Fig. 2 B, a marked reduction in the intracellular Cl^- concentration was observed in Ae4-transfected cells when the external $[Cl^-]$ was reduced (black circles). In contrast, no reduction in $[Cl^-]_i$ was observed upon external Cl^- reduction when external Na^+ was replaced by NMDG (Fig. 2 B, blue circles). Finally, as expected for a Cl^-/HCO_3^- exchange process,

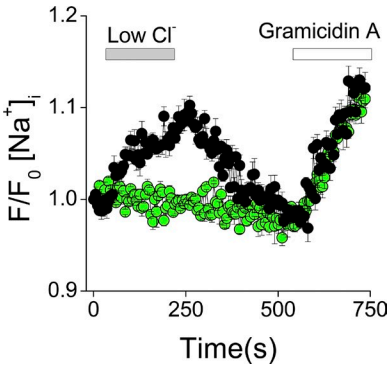

Figure 3. **Na^+ transport by the mouse Ae4 exchanger.** Intracellular Na^+ levels were estimated using the Na^+ indicator SBFI. A marked increase in intracellular [Na^+] was observed when the external [Cl^-] was reduced in Ae4-transfected (black circles; n = 15; changing solution A to B [Table 1]) but not in nontransfected (green circles; n = 13) cells. The increase in intracellular [Na^+] in Ae4-transfected cells was reversed by increasing the external [Cl^-] (changing solution B to A [Table 1]). Furthermore, addition of the Na^+-permeable ionophore gramicidin A at the end of the experiment demonstrated that SBFI was responsive to changes in intracellular Na^+. Results are presented as the mean ± SEM.

there was also no change in the $[Cl^-]_i$ in Ae4-transfected cells under HCO_3^--free conditions (Fig. 2 B, green circles).

Together, Fig. 2 (A and B) shows that both HCO_3^- uptake (alkalinization) and Cl^- loss (reduction in $[Cl^-]_i$) were prevented when external Na^+ was replaced by NMDG or in the absence of extracellular HCO_3^-, confirming that both HCO_3^- and Cl^- fluxes are tightly coupled to external Na^+. Similarly, Fig. 2 C shows that CHO-K1 cells expressing the human AE4 protein displayed Cl^-/HCO_3^- exchanger activity that was strongly dependent on extracellular Na^+, demonstrating that the Na^+ dependence displayed by mouse Ae4 is conserved in the human AE4 orthologue. A summary of the alkalinization rates calculated from experiments like those shown in Fig. 2 C (red lines) are presented in Fig. 2 D.

One possible explanation for the Na^+ dependence of Ae4-mediated anion transport is an allosteric modulation of Cl^-/HCO_3^- exchange by Na^+. Alternatively, Na^+ ions might be part of the Ae4-mediated transport cycle. To differentiate between these two possibilities, we measured changes in $[Na^+]_i$ using the Na^+ indicator SBFI. As seen in Fig. 3, an increase in $[Na^+]_i$ was observed when Cl^-/HCO_3^- exchange was activated by replacement of extracellular Cl^- with gluconate in Ae4-transfected CHO-K1 cells (black circles), but not in nontransfected cells (green circles), indicating that Ae4 mediates Na^+ transport. The increase in the $[Na^+]_i$ induced by extracellular Cl^- removal recovered to the initial $[Na^+]_i$ when extracellular Cl^- was restored, consistent with Na^+ moving in the opposite direction relative to Cl^- movement, although this could also be caused by Na^+/K^+-ATPase activity. Note that addition of the Na^+-permeable ionophore gramicidin A caused a rapid increase in the $[Na^+]_i$ in both Ae4-transfected and nontransfected CHO-K1 cells.

The Na^+ movement that accompanies Cl^-/HCO_3^- exchange could be an electroneutral or electrogenic transport process, depending on the stoichiometry of ions transported by Ae4. Simultaneous whole cell recordings (current clamp mode) and intracellular [Cl^-] measurements were performed to determine whether Ae4 activity is associated with changes in the membrane potential using pipette solution L (Table 2) supplemented with 1 mM of the Cl^- indicator SPQ. Under these experimental conditions, Ae4 expression in CHO-K1 cells caused a Na^+-dependent decrease in $[Cl^-]_i$ upon $[Cl^-]_o$ reduction (like Fig. 2 B results) that was essentially absent in nontransfected cells (Fig. 4 A). A summary of the Cl^- efflux rates calculated from experiments like those shown in Fig. 4 A (red lines) are presented in Fig. 4 B. In contrast, the whole cell current clamp measurements from the same cells shown in Fig. 4 A demonstrated that the activity of Ae4-mediated Na^+-dependent Cl^-/HCO_3^- exchange is an electroneutral process as little, if any, change in the membrane potential was associated with ion fluxes (Fig. 4 C); i.e., the change in the membrane potential was <2 mV when a low Cl^-, Na^+-free external solution (solution M in Table 2) was switched to a low Cl^-, Na^+-containing solution (solution N in Table 2). A summary of the change in the membrane potential calculated from experiments like those shown in Fig. 4 C are presented in Fig. 4 D. Additionally, we also evaluated the voltage dependence of Ae4-mediated transport in CHO-K1 cells using the voltage clamp whole cell configuration. By supplementing the pipette solution L (Table 2) with 100 μM of the pH indicator BCECF (free acid), we compared the Na^+-dependent alkalinization rates at −100 mV and 0 mV, respectively. As shown in Fig. 4 (E and F), an intracellular alkalinization was not observed in response to the addition of external Na^+ in nontransfected cells at −100 mV (black line, n = 5) or 0 mV (green line, n = 5). In contrast, Ae4-transfected cells displayed robust alkalinization rates at −100 mV (Fig. 4 E, black circles) and 0 mV (Fig. 4 E, green circles) that were essentially identical, supporting our findings obtained by current clamp whole cell recordings that showed the ion-transporting mechanism of Ae4 is electroneutral rather than electrogenic. Additionally, no differences in the macroscopic currents (voltage clamp experiments) were found in Ae4-transfected versus nontransfected cells. The difference in current before and after Na^+ addition to the external bath was −1.68 ± 0.44 pA/pF (n = 5) versus −1.27 ± 0.46 pA/pF (n = 5) at −100 mV (Ae4-transfected vs. nontransfected cells, P = 0.54, Student's t test) and −0.28 ± 0.09 pA/pF (n = 5) versus −0.21 ± 0.14 pA/pF (n = 5) at 0 mV, respectively (Ae4-transfected vs. nontransfected cells, P = 0.69, Student's t test).

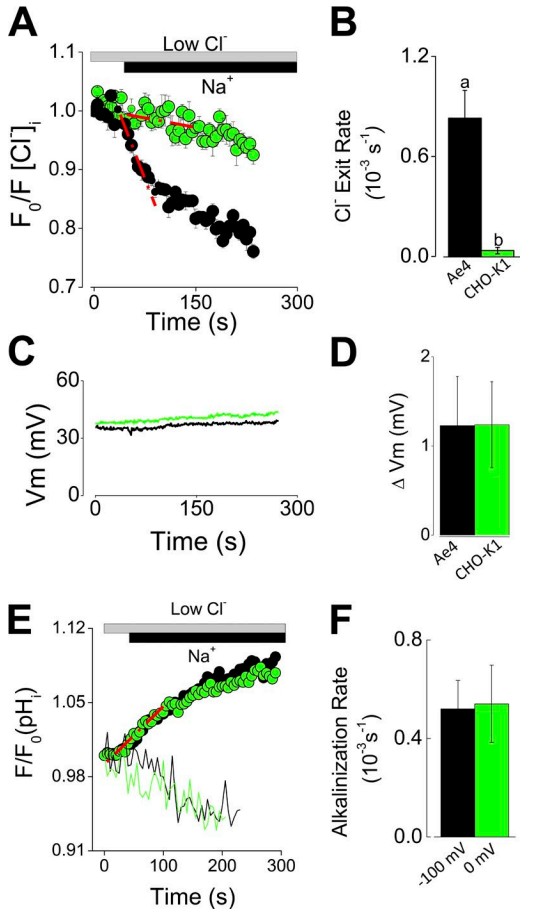

Figure 4. **Mouse Ae4 exchanger activity is not associated with changes in the membrane potential.** (A) Simultaneous current clamp whole cell recordings and $[Cl^-]_i$ measurements were performed on nontransfected (green circles) and Ae4-transfected cells (black circles) using a pipette solution containing 1 mM SPQ (solution L [Table 2]). The marked reduction in the intracellular $[Cl^-]$ in response to a decrease in the external Cl^- was used to confirm Ae4 expression in Ae4-transfected cells (change from solution M to N [Table 2]). (B) Summary of the Cl^- exit rates in nontransfected (green bar; $n = 8$) and Ae4-transfected cells (black bar; $n = 7$) calculated from linear regression analysis on the initial response to external Na^+ addition to the low Cl^- solution. Data are expressed as the mean ± SEM from single cells from at least three different electroporations. For Ae4, the black bar is significantly greater, "a" compared with "b" ($P < 0.01$, Student's *t* test). (C) Membrane potential measurements from the same cells shown in A in response to a reduction in the external Cl^- in nontransfected (green trace) and Ae4-transfected cells (black trace). (D) Summary of the changes in membrane potential measurements (obtained by subtracting the membrane potential values before and after reaching steady state in response to the addition of external Na^+) as shown in C. Results are presented as the mean ± SEM. (E) Simultaneous voltage clamp whole cell recordings and pH_i measurements were performed on Ae4-transfected cells at −100 mV (black circles; $n = 5$) and 0 mV (green circles; $n = 5$) using a pipette solution containing 100 µM BCECF (free acid; solution L [Table 2]). The marked increase in the pH_i in response to a decrease in the external Cl^- was used to confirm Ae4 expression in Ae4-transfected cells (change from solution M to N [Table 2]). No increase in pH_i upon external Cl^- reduction was observed in nontransfected cells held at −100 mV (black line; $n = 5$) and 0 mV (green line; $n = 5$), respectively. (F) Summary of the alkalinization rates displayed by Ae4-transfected cells held at −100 and 0 mV as shown in E. Data are expressed as the mean ± SEM from single cells from at least three different electroporations.

Does Ae4 mediate Na^+-HCO_3^- cotransport?

The aforementioned experiments indicate that Ae4 acts as an electroneutral, Na^+-dependent Cl^-/HCO_3^- exchanger, although others have suggested that Ae4 may also support Na^+-HCO_3^- cotransporter (NBC) activity (Chambrey et al., 2013). Consequently, we also tested whether Ae4 can mediate Na^+-HCO_3^- cotransporter activity in the absence of extracellular Cl^- (solutions G, H, and I in Table 1, containing 10 µM EIPA to inhibit the activity of endogenous Na^+/H^+ exchangers) to isolate NBC-like activity (Burnham et al., 1997). Fig. 5 shows that a rapid intracellular acidification was induced by perfusion with a HCO_3^-/CO_2-containing solution. In Ae4-expressing cells (Fig. 5, black circles), this acidification was dramatically blunted and then followed by a slower alkalinization that was absent in nontransfected cells (Fig. 5, green circles). Moreover, the Ae4-mediated intracellular alkalinization was tightly coupled to Na^+ transport as removal of external Na^+ prevented further alkalinization and caused an intracellular acidification.

The net Na^+-HCO_3^- cotransporter–like activity observed in Ae4-transfected cells under Cl^--free conditions (Fig. 5) could be the result of bona fide Na^+-HCO_3^- cotransport, Na^+-driven Cl^-/HCO_3^- exchange caused by incomplete intracellular Cl^- depletion or, alternatively, Na^+-driven HCO_3^-/HCO_3^- exchange where HCO_3^- substitutes for Cl^- in its absence. To differentiate between these possibilities, we used the whole cell (current clamp) configuration to control the intracellular ion composition while measuring the pH_i (low [HEPES], 1 mM, was included to permit the pH to change because of HCO_3^- influx). Ae4-mediated HCO_3^- influx was initiated by switching from a HCO_3^-/CO_2-free to a HCO_3^-/CO_2-containing external solution (conditions i and ii in Fig. 6 A, respectively) to induce an intracellular acidification, and then we compared the intracellular alkalinization rates after acidification. The external and pipette solutions were designed to impose a large inward Na^+ gradient to promote HCO_3^- influx.

To differentiate between Na^+-HCO_3^- cotransport and Na^+-driven HCO_3^-/HCO_3^- exchange using the protocol described in the previous paragraph, we then tested whether the Ae4-mediated alkalinization required intracellular HCO_3^- by comparing pipette solutions containing low Cl^- concentration with and without HCO_3^-. Fig. 6 A depicts two possible scenarios: Ae4-promoted HCO_3^- influx by a mechanism independent (cotransport) of or dependent (exchange) on intracellular HCO_3^-. Fig. 6 B shows that

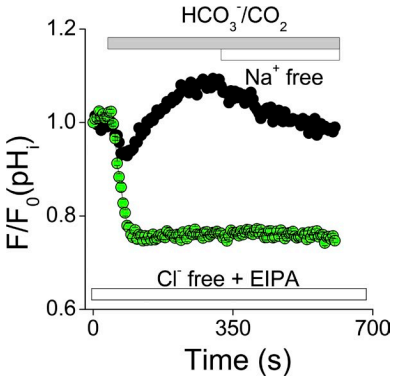

Figure 5. **Na^+-HCO_3^- cotransporter activity associated with mouse Ae4 expression under Cl^--free conditions.** Representative experiments showing pH_i measurements made in nontransfected (green circles; n = 14) and Ae4-transfected cells (black circles; n = 12) in response to a change in the external solution from a Na^+-containing HEPES-buffered to a Na^+-containing CO_2/HCO_3^--buffered solution (change from solution G to H [Table 1]). Then the external Na^+ was isotonically replaced by NMDG (change from solution H to I [Table 1]). The experiments were performed under Cl^--free conditions, and all solutions were supplemented with 10 µM EIPA to inhibit endogenous Na^+/H^+ exchanger activity. Results are presented as the mean ± SEM.

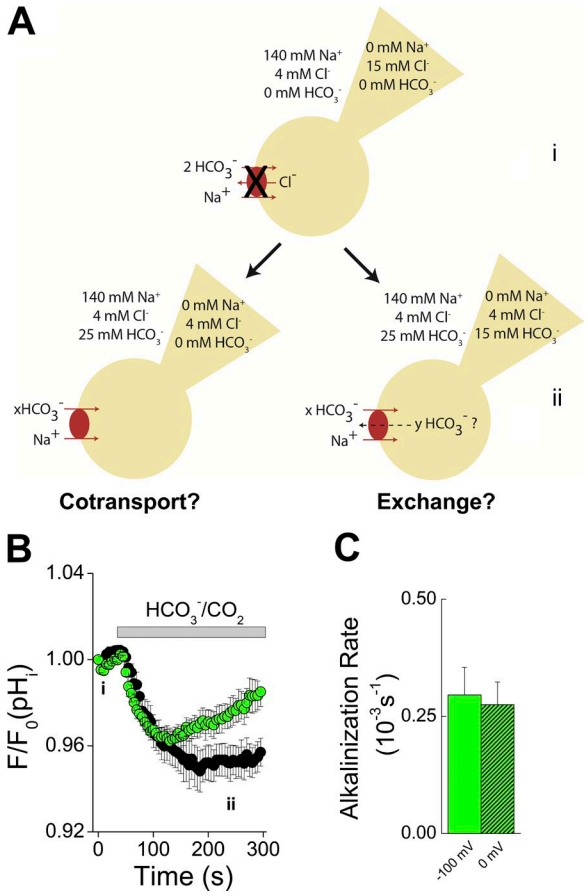

Figure 6. **Na^+-dependent HCO_3^-/HCO_3^- exchange under low Cl^- concentrations.** (A) Cartoon depicting the hypothetical Ae4-mediated HCO_3^- transport under low Cl^- concentrations when a HCO_3^--free external solution (condition i; solution R [Table 2]) was switched to a HCO_3^--containing external solution (condition ii; solution S [Table 2]). Note that there is no Ae4-mediated transport under HCO_3^--free conditions. Furthermore, given that the stoichiometric coefficients of Ae4-mediated HCO_3^- transport under low Cl^- conditions are unknown, we have denoted them as x (extracellular) and y (intracellular), respectively. (B) A decrease in the pH_i was observed after the external HEPES-buffered solution was replaced with a CO_2/HCO_3^--buffered solution (change of solution R to S [Table 2]). Little, if any, alkalinization was observed in Ae4-transfected cells using a HCO_3^--free pipette solution containing low Cl^- (4 mM; black circles; n = 6; solution P [Table 2]). In contrast, the initial acidification was followed by a marked intracellular alkalinization in Ae4-transfected cells dialyzed with a pipette solution containing 15 mM HCO_3^- + 4 mM Cl^- (green circles; n = 7; solution Q [Table 2]). A summary of the results calculated from experiments shown in this figure is given in Table 4. Results are presented as the mean ± SEM. (C) Summary of the alkalinization rates obtained in response to intracellular acidification from Ae4-transfected cells (voltage clamp whole cell recordings) held at −100 mV (green bar; n = 5) and 0 mV (green dashed bar; n = 4) using a HCO_3^--containing pipette solution supplemented with 100 µM BCECF (free acid; solution Q [Table 2]). Data are expressed as the mean ± SEM from single cells from at least three different electroporations.

little if any intracellular alkalinization occurred in response to the HCO_3^-/CO_2-induced acidification in Ae4-transfected cells dialyzed with a HCO_3^--free pipette solution (black circles; solution P in Table 2). Conversely, a distinct alkalinization was seen with a pipette solution containing 15 mM HCO_3^- (Fig. 6 B, green circles; solution Q in Table 2). Furthermore, there were no differences in the membrane potential changes between nontransfected and Ae4-transfected cells under these experimental conditions. Table 4 summarizes results obtained in experiments like those shown in Fig. 6 and also includes the membrane potential measurements recorded from nontransfected cells using the same pipette solutions. Additionally, we evaluated the voltage dependence of the intracellular alkalinization observed when a pipette solution containing 15 mM HCO_3^- supplemented with BCECF (free acid) was used. As shown in Fig. 6 C, voltage clamp whole cell recordings showed that the alkalinization rates were essentially identical in Ae4-expressing cells held at −100 mV and 0 mV, respectively. Additionally, the difference in the macroscopic currents (normalized by capacitance) before and after switching from HEPES-buffered to a CO_2-HCO_3^-–buffered solution did not differ between Ae4-transfected versus nontransfected cells; the values were −2.60 ± 1.39 pA/pF (n = 5) versus −0.90 ± 0.64 pA/pF (n = 4) at −100 mV (Ae4-transfected vs. nontransfected, P = 0.34, Student's t test) and 0.31 ± 0.17 pA/pF (n = 4) vs. 0.41 ± 0.07 pA/pF (n = 4) at 0 mV (Ae4-transfected vs. nontransfected, P = 0.58, Student's t test). Collectively, these results indicate that the Ae4-mediated alkalinization can be driven by intracellular HCO_3^-,

Table 4. **Results obtained from simultaneous pH and membrane potential measurements**

Pipette solutions	Ae4-transfected cells			Nontransfected cells		
	Alkalinization rate	ΔVm	*n*	Alkalinization rate	ΔVm	*n*
	10^{-3} s^{-1}	*mV*		10^{-3} s^{-1}	*mV*	
O (Cl^- containing)	0.12 ± 0.03	−15.6 ± 2	6	ND	−16.5 ± 2	5
P (HCO_3^- free)	0.02 ± 0.01[a,b]	−16.2 ± 2	6	ND	−15.8 ± 1	4
Q (HCO_3^- containing)	0.08 ± 0.01	−20.0 ± 3	7	ND	−16.1 ± 3	4

[a]P is different from O pipette solution, P = 0.01 (ANOVA).
[b]P is different from Q pipette solution, P = 0.001.

which is not consistent with Na^+-HCO_3^- cotransport activity, but with an electroneutral, Na^+-driven Cl^-/HCO_3^- exchange where HCO_3^- substitutes for Cl^- in its absence (HCO_3^-/HCO_3^- exchange). In fact, given that Ae4 transport is electroneutral, the efficiency of intracellular HCO_3^- to promote Na^+-2 HCO_3^- influx is similar to that displayed by intracellular Cl^-; i.e., the alkalinization rates were not significantly different between pipette solutions containing either 15 mM HCO_3^- + 4 mM Cl^- (solution Q in Table 2) or a HCO_3^--free pipette solution containing 15 mM Cl^- (solution O in Table 2; results obtained under this condition are included in Table 4).

Cation selectivity of Ae4

Salivary gland acinar cells that lack Ae4 (*Ae4*$^{-/-}$) display a lower resting state $[Cl^-]_i$ and secrete less agonist-induced saliva compared with wild-type control glands (Peña-Münzenmayer et al., 2015). These observations suggest that Ae4 acts as a Cl^- concentrative pathway that is important for stimulated Cl^--dependent fluid secretion and raise questions about the physiological transport mechanism by which Ae4 promotes Cl^- influx and $NaHCO_3$ efflux. Given that Ae4-mediated transport is an electroneutral process (see Fig. 4) and assuming the following fixed steady-state ion concentrations for SMG acinar cells (mM):

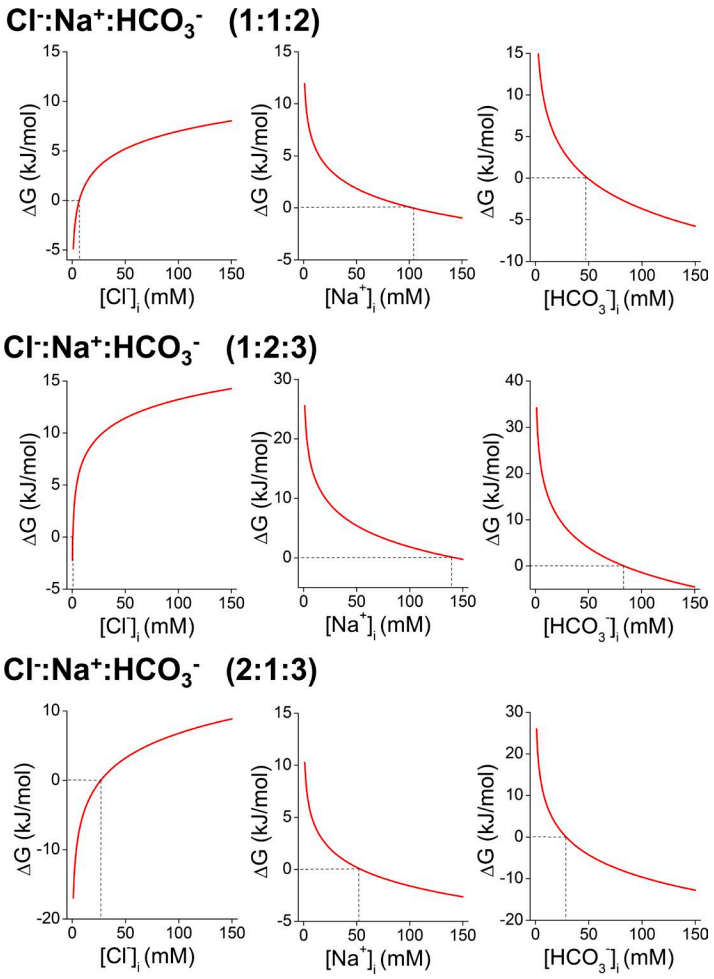

Figure 7. **Predicted changes in ΔG associated with Ae4 activity.** ΔG values calculated for Ae4 transport activity assuming stoichiometries of Cl^-:Na^+:HCO_3^- as 1:1:2 (top row), 1:2:3 (middle row), and 2:1:3 (bottom row), respectively. The intracellular Cl^- (left column), Na^+ (middle column), and HCO_3^- (right column) were individually changed (from 0.5 to 150 mM) while the other concentrations were kept fixed at $[Cl^-]_i$ = 50.1 mM, $[Na^+]_i$ = 15.5 mM, or $[HCO_3^-]_i$ = 19 mM.

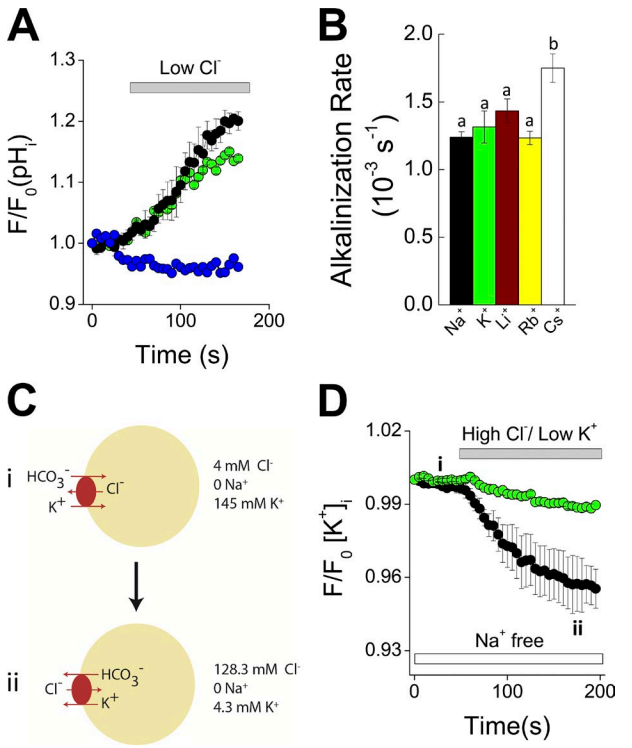

Figure 8. **Cation selectivity of Ae4.** (A) Changes in pH_i seen in response to a reduction in the external $[Cl^-]$ was tested in Ae4-transfected cells when Na^+ (black circles; n = 10; change from solution A to B [Table 1]), K^+ (green circles; n = 8; change from solution J to K [Table 1]), or NMDG (blue circles; n = 6; change from solution C to D [Table 1]) was the main cation in the external solutions. (B) Summary of experiments shown in A for Na^+ and K^+, as well as those with external solutions containing Rb^+ (n = 6), Li^+ (n = 6), and Cs^+ (n = 6; 100 mM each; see solutions Rb^+ 100, Li^+ 100, and Cs^+ 100 in Table 3). For Cs^+, the white bar is significantly greater, "a" compared with "b" ($P < 0.05$, one-way ANOVA followed by Bonferroni's post hoc test). (C) Cartoon depicting the experimental design used to evaluate K^+ transport by Ae4. (D) Nontransfected (green circles; n = 8) and Ae4-transfected cells (black circles; n = 6) loaded with the K^+ indicator PBFI-AM were initially depleted of Cl^- by incubating the cells with a low Cl^- (solution K [Table 1]) and then Cl^- uptake activated by switching to an external solution containing high Cl^- (solution C [Table 1]). The experiment was conducted under Na^+-free conditions to prevent Na^+ contamination of the PBFI signal. (A, B, and D) Results are presented as the mean ± SEM.

$[Cl^-]_o$ = 124.6 (Mangos et al., 1973), $[Cl^-]_i$ = 50.1 (Peña-Münzenmayer et al., 2015), $[HCO_3^-]_o$ = 24.7 (serum; Mangos et al., 1973), $[HCO_3^-]_i$ = 19 (calculated; Patterson et al., 2012), $[Na^+]_o$ = 151.6 (Mangos et al., 1973), and $[Na^+]_i$ = 15.5 (calculated from rat sublingual acini; Zhang et al., 1993), we calculated the Gibbs free energy (ΔG) values that are associated with Ae4-mediated Cl^- influx by independently varying the intracellular concentrations of Cl^-, Na^+, and HCO_3^-, respectively. ΔG values were obtained assuming the following potential stoichiometries that could produce electroneutral Ae4-mediated transport (Cl^-:Na^+:HCO_3^-): 1:1:2, 1:2:3, and 2:1:3 (Eqs. 1, 2, and 3 in Materials and methods). Fig. 7 shows that intracellular Cl^- concentrations <7 mM at 1:1:2 (top left graph), 0.5 mM at 1:2:3 (middle left graph), and 26 mM at 2:1:3 (bottom left graph) stoichiometries, respectively, are required to reach the negative ΔG values that thermodynamically favor an Ae4-mediated Cl^- influx. The calculated intracellular Na^+ concentrations (middle row) required to reach negative ΔG values and favor Ae4-mediated Cl^- influx are predicted to be >104 mM at 1:1:2 (top), 143 mM at 1:2:3 (middle), and 54 mM at 2:1:3 (bottom). The right panels show that $[HCO_3^-]_i$ >49 mM (1:1:2; top right), 84 mM (1:2:3, middle right), and 29 mM (2:1:3, bottom right) are required to reach negative ΔG values to promote Ae4-mediated Cl^- influx.

Because the intracellular Cl^-, Na^+, and HCO_3^- concentrations required to achieve negative ΔG values are quite far from the intracellular Cl^-, Na^+, and HCO_3^- concentrations reported for salivary gland acinar cells at rest and even during sustained stimulation, it seems unlikely that Na^+ is the physiologically relevant cation. Thus, we hypothesized that K^+, the main intracellular monovalent cation, supports Ae4-mediated Cl^-/HCO_3^- exchange. Fig. 8 A shows that a substantial intracellular alkalinization was evoked in Ae4-transfected cells in response to a reduction in $[Cl^-]_o$ in both Na^+ (black circles)- and K^+ (green circles)-containing external solutions. In contrast, an intracellular alkalinization was not induced by low $[Cl^-]_o$ in Ae4-transfected cells when NMDG was the main external cation (Fig. 8 A, blue circles). Moreover, Fig. 8 B shows that the selectivity of the cation-dependent transport of Ae4 poorly distinguishes between the monovalent inorganic cations Na^+, K^+, Li^+, Rb^+, and Cs^+; all tested cations evoked a robust Cl^-/HCO_3^- exchange in Ae4-transfected cells.

The aforementioned results strongly suggest that like Na^+, K^+ and other monovalent cations may be transported by Ae4. To directly test whether K^+ is transported by Ae4, the K^+-selective probe PBFI was used to measure $[K^+]_i$ during stimulated Ae4 activity. Given that PBFI is only ∼1.5-times more selective for K^+ than Na^+ ions, we performed these experiments under Na^+-free conditions to eliminate Na^+ contamination of the K^+ signal (Minta and Tsien, 1989). The experimental design is shown in Fig. 8 C. In brief, cells were loaded with PBFI and then perfused with a low $[Cl^-]$, Na^+-free/high $[K^+]$ external solution to deplete the cells of Cl^- (Fig. 8, C and D, condition i). If Ae4 transports K^+, then it would be expected that a combination of inwardly directed Cl^- and outwardly directed K^+ gradients (by increasing $[Cl^-]_o$ and decreasing $[K^+]_o$) would promote Cl^- influx in exchange for K^+ (and HCO_3^-) efflux, respectively (Fig. 8, C and D, condition ii). Fig. 8 D shows that a sustained reduction in the $[K^+]_i$ was observed when inward-directed Cl^- and out-

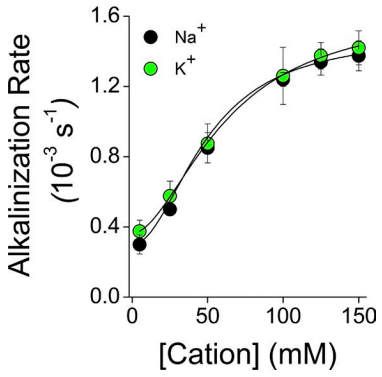

Figure 9. **Dependence of Ae4 activity on external Na^+ and K^+ concentrations.** Ae4 activity was measured as the alkalinization rate in response to a reduction in the external [Cl^-] using Na^+- and K^+-containing solutions (change from solution A in Table 1 to external solutions 5, 25, 50, 100, 125, and 150 mM [see Table 3 for ion composition of the Na^+- and K^+-containing solutions]). The calculated activities at different cation concentrations were plotted against the cation concentration and then fitted to a Hill function as described in Materials and methods, Eq. 4. The Hill fits are plotted as black lines. Data are expressed as the mean ± SEM from at least four experiments per condition that included at least three different electroporations.

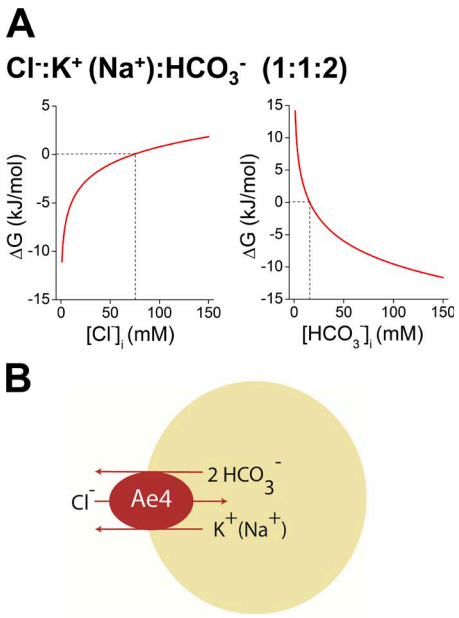

Figure 10. **Predicted changes in ΔG associated with Ae4 transport assuming that the cation transport pathway does not distinguish between Na^+ and K^+.** (A) ΔG values calculated assuming a 1:1:2 stoichiometry of Cl^-:K^+ (Na^+):HCO_3^-. The intracellular Cl^- (left) and HCO_3^- (right) were individually changed (from 0.5 to 150 mM) while the other concentrations were kept fixed at either $[Cl^-]_i$ = 50.1 mM or $[HCO_3^-]_i$ = 19 mM. (B) Proposed model for Ae4-mediated Cl^- uptake in secretory acinar cells.

ward-directed K^+ gradients were imposed to Ae4-transfected cells, but little, if any, K^+ efflux was observed in nontransfected cells, strongly suggesting that Ae4 indeed transports K^+ ions. Dose–response experiments revealed that the affinities of Ae4 for Na^+ and K^+ ions were comparable (Fig. 9), where the EC_{50} values for Na^+ and K^+ were 49 mM and 62 mM, respectively. The R_{Min}, R_{Max}, and nH obtained from Hill's function fittings (see Eq. 4 in Materials and methods) to the data shown in Fig. 9 were 0.3, 1.5, and 2.0 for Na^+ and 0.4, 1.6, and 1.8 for K^+, respectively.

Assuming that physiological $[Na^+]_i + [K^+]_i \approx [Na^+]_o + [K^+]_o$ and that Ae4 nearly equally transports Na^+ and K^+ (Fig. 9), we calculated ΔG associated with a stoichiometry of 1:1:2 [Cl^-:K^+(Na^+):HCO_3^-]. Considering the aforementioned premises, it can be inferred from Eq. 1 that the Na^+ and K^+ gradients do not influence the direction of the Ae4-mediated transport. Therefore, the direction of the ion transport mediated by Ae4 will be governed by the Cl^- and HCO_3^- gradients. Using the same ion concentrations for the ΔG values shown in Fig. 7, the changes in ΔG value at different $[Cl^-]_i$ and $[HCO_3^-]_i$ were calculated. As shown in Fig. 10 A, a $[Cl^-]_i$ <73 mM (left graph) and a $[HCO_3^-]_i$ >16 mM (right graph) are sufficient to support Cl^- uptake by Ae4, ion concentrations that are in agreement with the physiological concentration range estimated for Cl^- and HCO_3^- in secretory acinar cells, 51.1 and 19 mM, respectively. Finally, a working model for Ae4 mediating Cl^- influx in exchange for K^+(Na^+)HCO_3 (efflux) in acinar secretory cells is shown in Fig. 10 B.

DISCUSSION

To better understand the physiological role of Ae4 in the kidney, exocrine glands and other tissues, it is essential to determine the ion transport mechanism underlying Ae4 function. The first cloning studies reported that rabbit (kidney β-intercalated cells; Tsuganezawa et al., 2001) and rat (kidney cDNA library; Ko et al., 2002) Ae4 orthologues are Na^+-independent Cl^-/HCO_3^- exchangers. In contrast, Chambrey et al. (2013) suggested that Ae4 is a Na^+-HCO_3^- cotransporter in mouse kidney β-intercalated cells, whereas the Ae4 expressed in mouse salivary gland acinar cells appears to act as a Na^+-dependent Cl^-/HCO_3^- exchanger; however, detailed characterization of the Ae4-mediated ion transport mechanism was not performed (Peña-Münzenmayer et al., 2015). Thus, the aim of the present study was to gain further insight into the Ae4-mediated ion transport mechanism. We took advantage of *Ae2*$^{-/-}$ mice to study the native Ae4 Cl^-/HCO_3^- exchanger activity expressed in salivary gland acinar cells. A large Ae4-mediated intracellular alkalinization in response to a reduction in external [Cl^-] that was dependent on external Na^+ was observed in acinar cells. This response was not present in acinar cells from glands lacking both Ae2 and Ae4, confirming that the remaining activity in *Ae2*$^{-/-}$ acinar cells corresponds to Ae4-mediated Na^+-dependent Cl^-/

HCO_3^- exchange. Moreover, CHO-K1 cells expressing mouse Ae4 and human AE4 cDNAs mimicked the results obtained in native acinar cells. Collectively, our results demonstrate that both native and recombinant Ae4 act as Na^+-dependent Cl^-/HCO_3^- exchangers, although Na^+-dependent Cl^-/CO_3^{2-} exchange activity cannot be ruled out.

We next explored the nature of the Na^+ dependence of Ae4-mediated Cl^-/HCO_3^- exchange by addressing two basic questions: is the Na^+ dependence caused by an allosteric modulation of Cl^-/HCO_3^- exchange or is Ae4 able to transport Na^+ ions? Consistent with the hypothesis that Ae4 activity is associated with Na^+ transport, we found that Ae4-mediated HCO_3^- influx was accompanied by an increase in the intracellular $[Na^+]$. Moreover, Ae4 activity did not generate a change in the membrane potential, demonstrating that Ae4 mediates an electroneutral, Na^+ transport-dependent exchange of Cl^- and HCO_3^-.

We also found that Ae4 can produce net Na^+-HCO_3^- cotransport under nonphysiological Cl^--free conditions. Simultaneous whole cell recordings and pH_i measurements revealed that Na^+-coupled HCO_3^- influx occurred with either Cl^- or HCO_3^- as the primary intracellular permeable anion, whereas little or no HCO_3^- influx was observed in a HCO_3^--free, low Cl^-–containing pipette solution (Table 4). Moreover, there was no difference in the change of the membrane potential between Ae4-tranfected and nontransfected cells in response to HCO_3^-/CO_2-induced acidification. Voltage clamp experiments comparing Ae4 activity at −100 and 0 mV showed no voltage dependence of Ae4-mediated ion transport, consistent with Ae4 mediating both electroneutral $Cl^-/NaHCO_3$ or $HCO_3^-/NaHCO_3$ exchange; however, we cannot rule out that OH^- ions can substitute for Cl^- ions and mediate $OH^-/NaHCO_3$ exchange. Although our findings differ from those reported by Chambrey et al. (2013) regarding the activity encoded by Ae4 (i.e., $Cl^-/NaHCO_3$ exchange vs. $NaHCO_3$ cotransport), both studies are in agreement with Na^+ ions being transported by Ae4 in the same direction as HCO_3^- ions. A detailed characterization of the Cl^- dependence of Ae4-mediated activity in β-intercalated cells is required to evaluate whether the ion-transporting mechanism by Ae4 differs or is conserved in salivary glands and kidney, respectively.

Epithelial fluid secretion is a Cl^--dependent process in which basolateral Cl^- uptake and apical Cl^- efflux pathways are required to promote vectorial Cl^- secretion into the luminal space (Silva et al., 1977; Greger, 2000). The electroneutral basolateral Na^+-K^+-$2Cl^-$ cotransporter (NKCC1) is the major Cl^- concentrative pathway in several tissues (Kunzelmann and Mall, 2002; Melvin et al., 2005), but a HCO_3^--dependent Cl^- concentrative mechanism has also proven to be important for secretion in many epithelia, including the duodenum and salivary glands (Walker et al., 2002; Peña-Münzenmayer et al., 2015). In fact, we found that salivary glands lacking the HCO_3^- transporter Ae4 (*Ae4*$^{-/-}$) display impaired fluid secretion as well as a lower $[Cl^-]_i$ in their acinar cells (Peña-Münzenmayer et al., 2015), suggesting that Ae4 is involved in a Cl^- concentrative pathway. If Ae4 indeed mediates Cl^- influx in acinar cells by promoting $Cl^-/NaHCO_3$ exchange with a stoichiometry of 1:1:2 (Cl^-, Na^+, and HCO_3^-), ΔG calculations predict that Ae4 mediates Cl^- efflux rather than Cl^- influx under physiological conditions. One possible explanation for the inconsistency between experimental data obtained from the *Ae4*$^{-/-}$ mouse and the thermodynamic calculations could be off-target effects on the expression of another Cl^--uptake pathway. However, this seems unlikely because the Nkcc1 Na^+-K^+-$2Cl^-$ cotransporter activity was not affected by *Ae4* gene disruption (Peña-Münzenmayer et al., 2015). Alternatively, Ae4 could promote Cl^- influx and HCO_3^- efflux by another ion transport mechanism. To test this possibility, we considered whether the Na^+ transport pathway of Ae4 might display cation promiscuity and, therefore, K^+ might substitute for Na^+ to promote Cl^-/HCO_3^- exchange. We found that Ae4 expression promotes K^+-dependent Cl^-/HCO_3^- exchange and K^+ efflux when an inward directed Cl^- gradient is imposed. Together, these results strongly suggest that Ae4 is able to transport both K^+ and Na^+ ions, and in fact, the cation transport pathway of Ae4 appears be nonselective as Li^+, Rb^+, and Cs^+ ions also drive Ae4-mediated Cl^-/HCO_3^- exchange.

Dose–response experiments for Na^+ and K^+ ions found that these two cations share almost identical EC_{50}, maximal alkalinization rates (R_{Max}), and Hill (*nH*) values obtained from Hill plots. The *nH* values obtained for Na^+ and K^+ (2.0 and 1.8, respectively) show that Na^+ and K^+ ions exert a cooperative effect on Ae4 activity. This finding suggests that (a) more than one Na^+ or K^+ ion is transported per cycle by Ae4 where the binding of the first cation facilitates the binding of another cation or (b) in addition to Ae4-mediated cation transport, Na^+ or K^+ ions may allosterically regulate Ae4 activity. More experiments in the future are required to address this open question.

Given that the sum of the external Na^+ and K^+ concentrations is nearly identical to the sum of intracellular Na^+ and K^+ concentrations, it can be inferred that the direction of the Cl^- and HCO_3^- transport by Ae4 is governed by the Cl^- and HCO_3^- chemical gradients; that is, the sum of the inward and outward cation driving forces cancel out. Further ΔG calculations assuming a stoichiometry of Cl^-:$K^+(Na^+)$:HCO_3^- of 1:1:2 (when $[Cl^-]_o$ = 124.6 mM, $[Cl^-]_i$ = 50.1 mM, $[HCO_3^-]_o$ = 24.7 mM, and $[HCO_3^-]_i$ = 19 mM, both $[Na^+]_o + [K^+]_o$ and $[Na^+]_i + [K^+]_i$ = 155 mM) confirm that the ΔG values are negative for Ae4-mediated Cl^- influx at the Cl^- and HCO_3^- concen-

trations reported for acinar secretory cells at rest, supporting a critical role of Ae4 in accumulating Cl^- above its equilibrium potential in exchange for HCO_3^- efflux in acinar cells. In addition to basolateral K^+ channels, the K^+ permeability displayed by Ae4 might also be important as a K^+ recycling pathway to support Na^+/K^+ ATPase activity under some physiological conditions.

In summary, the present study provides evidence for the first time of a nonselective cationic transport pathway in a member of the Slc4a family of HCO_3^- transporters. Importantly, the cationic nonselectivity displayed by Ae4 might be shared with other Na^+-dependent members of the Slc4a family, and thus, these transporters may play physiological roles different than those previously predicted. For instance, the electroneutral K^+-HCO_3^- cotransporter activity described in the kidney (Leviel et al., 1992; Blanchard et al., 1996) as well as in other species (Hogan et al., 1995a,b; Zhao et al., 1995) might be encoded by a member of the *Slc4a* family.

ACKNOWLEDGMENTS

We thank Drs. Z. Borok, E.D. Crandall, and U.P. Flodby for kindly providing the Aqp5-Cre (ACID) mice.

This study was supported by the Intramural Research Program of the National Institute of Dental and Craniofacial Research, National Institutes of Health (NIH; to J.E. Melvin) and NIH grant DK050594 (to G.E. Shull).

The authors declare no competing financial interests.

Merritt Maduke served as editor.

Submitted: 12 January 2016
Accepted: 5 April 2016

REFERENCES

Barry, P.H. 1994. JPCalc, a software package for calculating liquid junction potential corrections in patch-clamp, intracellular, epithelial and bilayer measurements and for correcting junction potential measurements. *J. Neurosci. Methods.* 51:107–116. http://dx.doi.org/10.1016/0165-0270(94)90031-0

Blanchard, A., F. leviel, M. Bichara, R.A. Podevin, and M. Paillard. 1996. Interactions of external and internal K^+ with K^+-HCO_3^- cotransporter of rat medullary thick ascending limb. *Am. J. Physiol.* 271:C218–C225.

Burnham, C.E., H. Amlal, Z. Wang, G.E. Shull, and M. Soleimani. 1997. Cloning and functional expression of a human kidney Na+:HCO3- cotransporter. *J. Biol. Chem.* 272:19111–19114. http://dx.doi.org/10.1074/jbc.272.31.19111

Chambrey, R., I. Kurth, J. Peti-Peterdi, P. Houillier, J.M. Purkerson, F. Leviel, M. Hentschke, A.A. Zdebik, G.J. Schwartz, C.A. Hübner, and D. Eladari. 2013. Renal intercalated cells are rather energized by a proton than a sodium pump. *Proc. Natl. Acad. Sci. USA.* 110:7928–7933. http://dx.doi.org/10.1073/pnas.1221496110

Chao, A.C., J.A. Dix, M.C. Sellers, and A.S. Verkman. 1989. Fluorescence measurement of chloride transport in monolayer cultured cells. Mechanisms of chloride transport in fibroblasts. *Biophys. J.* 56:1071–1081. http://dx.doi.org/10.1016/S0006-3495(89)82755-9

Coury, F., S. Zenger, A.K. Stewart, S. Stephens, L. Neff, K. Tsang, G.E. Shull, S.L. Alper, R. Baron, and A.O. Aliprantis. 2013. SLC4A2-mediated Cl^-/HCO_3^- exchange activity is essential for calpain-dependent regulation of the actin cytoskeleton in osteoclasts. *Proc. Natl. Acad. Sci. USA.* 110:2163–2168. http://dx.doi.org/10.1073/pnas.1206392110

Flodby, P., Z. Borok, A. Banfalvi, B. Zhou, D. Gao, P. Minoo, D.K. Ann, E.E. Morrisey, and E.D. Crandall. 2010. Directed expression of Cre in alveolar epithelial type 1 cells. *Am. J. Respir. Cell Mol. Biol.* 43:173–178. http://dx.doi.org/10.1165/rcmb.2009-0226OC

Gawenis, L.R., E.M. Bradford, V. Prasad, J.N. Lorenz, J.E. Simpson, L.L. Clarke, A.L. Woo, C. Grisham, L.P. Sanford, T. Doetschman, et al. 2007. Colonic anion secretory defects and metabolic acidosis in mice lacking the NBC1 Na^+/HCO_3^- cotransporter. *J. Biol. Chem.* 282:9042–9052. http://dx.doi.org/10.1074/jbc.M607041200

Greger, R. 2000. Role of CFTR in the colon. *Annu. Rev. Physiol.* 62:467–491. http://dx.doi.org/10.1146/annurev.physiol.62.1.467

Grichtchenko, I.I., I. Choi, X. Zhong, P. Bray-Ward, J.M. Russell, and W.F. Boron. 2001. Cloning, characterization, and chromosomal mapping of a human electroneutral Na^+-driven Cl-HCO_3 exchanger. *J. Biol. Chem.* 276:8358–8363. http://dx.doi.org/10.1074/jbc.C000716200

Hogan, E.M., M.A. Cohen, and W.F. Boron. 1995a. K^+- and HCO_3^--dependent acid-base transport in squid giant axons II. Base influx. *J. Gen. Physiol.* 106:845–862. http://dx.doi.org/10.1085/jgp.106.5.845

Hogan, E.M., M.A. Cohen, and W.F. Boron. 1995b. K^+- and HCO_3^--dependent acid-base transport in squid giant axons. I. Base efflux. *J. Gen. Physiol.* 106:821–844. http://dx.doi.org/10.1085/jgp.106.5.821

Illsley, N.P., and A.S. Verkman. 1987. Membrane chloride transport measured using a chloride-sensitive fluorescent probe. *Biochemistry.* 26:1215–1219. http://dx.doi.org/10.1021/bi00379a002

Ishiguro, H., M.C. Steward, A.R. Lindsay, and R.M. Case. 1996. Accumulation of intracellular HCO3- by Na(+)-HCO3- cotransport in interlobular ducts from guinea-pig pancreas. *J. Physiol.* 495:169–178. http://dx.doi.org/10.1113/jphysiol.1996.sp021582

Kao, L., R. Azimov, N. Abuladze, D. Newman, and I. Kurtz. 2015. Human SLC4A11-C functions as a DIDS-stimulatable $H^+(OH^-)$ permeation pathway: partial correction of R109H mutant transport. *Am. J. Physiol. Cell Physiol.* 308:C176–C188. http://dx.doi.org/10.1152/ajpcell.00271.2014

Ko, S.B.H., X. Luo, H. Hager, A. Rojek, J.Y. Choi, C. Licht, M. Suzuki, S. Muallem, S. Nielsen, and K. Ishibashi. 2002. AE4 is a DIDS-sensitive Cl^-/HCO_3^- exchanger in the basolateral membrane of the renal CCD and the SMG duct. *Am. J. Physiol. Cell Physiol.* 283:C1206–C1218. http://dx.doi.org/10.1152/ajpcell.00512.2001

Kunzelmann, K., and M. Mall. 2002. Electrolyte transport in the mammalian colon: mechanisms and implications for disease. *Physiol. Rev.* 82:245–289. http://dx.doi.org/10.1152/physrev.00026.2001

Leviel, F., P. Borensztein, P. Houillier, M. Paillard, and M. Bichara. 1992. Electroneutral K+/HCO3- cotransport in cells of medullary thick ascending limb of rat kidney. *J. Clin. Invest.* 90:869–878. http://dx.doi.org/10.1172/JCI115962

Leviel, F., C.A. Hübner, P. Houillier, L. Morla, S. El Moghrabi, G. Brideau, H. Hassan, M.D. Parker, I. Kurth, A. Kougioumtzes, et al. 2010. The Na^+-dependent chloride-bicarbonate exchanger SLC4A8 mediates an electroneutral Na^+ reabsorption process in the renal cortical collecting ducts of mice. *J. Clin. Invest.* 120:1627–1635. (published erratum appears in *J. Clin. Invest.* 2011. 121:1668) http://dx.doi.org/10.1172/JCI40145

Mangos, J.A., N.R. McSherry, S. Nousia-Arvanitakis, and K. Irwin. 1973. Secretion and transductal fluxes of ions in exocrine glands of the mouse. *Am. J. Physiol.* 225:18–24.

Melvin, J.E., D. Yule, T. Shuttleworth, and T. Begenisich. 2005. Regulation of fluid and electrolyte secretion in salivary gland acinar cells. *Annu. Rev. Physiol.* 67:445–469. http://dx.doi.org/10.1146/annurev.physiol.67.041703.084745

Minta, A., and R.Y. Tsien. 1989. Fluorescent indicators for cytosolic sodium. *J. Biol. Chem.* 264:19449–19457.

Nguyen, H.V., A. Stuart-Tilley, S.L. Alper, and J.E. Melvin. 2004. Cl^-/HCO_3^- exchange is acetazolamide sensitive and activated by a muscarinic receptor-induced $[Ca^{2+}]_i$ increase in salivary acinar cells. *Am. J. Physiol. Gastrointest. Liver Physiol.* 286:G312–G320. http://dx.doi.org/10.1152/ajpgi.00158.2003

Ogando, D.G., S.S. Jalimarada, W. Zhang, E.N. Vithana, and J.A. Bonanno. 2013. SLC4A11 is an EIPA-sensitive Na^+ permeable pH_i regulator. *Am. J. Physiol. Cell Physiol.* 305:C716–C727. http://dx.doi.org/10.1152/ajpcell.00056.2013

Park, M., Q. Li, N. Shcheynikov, W. Zeng, and S. Muallem. 2004. NaBC1 is a ubiquitous electrogenic Na^+-coupled borate transporter essential for cellular boron homeostasis and cell growth and proliferation. *Mol. Cell.* 16:331–341. http://dx.doi.org/10.1016/j.molcel.2004.09.030

Parker, M.D., and W.F. Boron. 2013. The divergence, actions, roles, and relatives of sodium-coupled bicarbonate transporters. *Physiol. Rev.* 93:803–959. http://dx.doi.org/10.1152/physrev.00023.2012

Parker, M.D., R. Musa-Aziz, J.D. Rojas, I. Choi, C.M. Daly, and W.F. Boron. 2008. Characterization of human SLC4A10 as an electroneutral Na/HCO_3 cotransporter (NBCn2) with Cl^- self-exchange activity. *J. Biol. Chem.* 283:12777–12788. http://dx.doi.org/10.1074/jbc.M707829200

Patterson, K., M.A. Catalán, J.E. Melvin, D.I. Yule, E.J. Crampin, and J. Sneyd. 2012. A quantitative analysis of electrolyte exchange in the salivary duct. *Am. J. Physiol. Gastrointest. Liver Physiol.* 303:G1153–G1163. http://dx.doi.org/10.1152/ajpgi.00364.2011

Peña-Münzenmayer, G., M.A. Catalán, Y. Kondo, Y. Jaramillo, F. Liu, G.E. Shull, and J.E. Melvin. 2015. Ae4 (Slc4a9) anion exchanger drives Cl^- uptake-dependent fluid secretion by mouse submandibular gland acinar cells. *J. Biol. Chem.* 290:10677–10688. http://dx.doi.org/10.1074/jbc.M114.612895

Rink, T.J., R.Y. Tsien, and T. Pozzan. 1982. Cytoplasmic pH and free Mg2+ in lymphocytes. *J. Cell Biol.* 95:189–196. http://dx.doi.org/10.1083/jcb.95.1.189

Romero, M.F., A.-P.P. Chen, M.D. Parker, and W.F. Boron. 2013. The SLC4 family of bicarbonate (HCO_3^-) transporters. *Mol. Aspects Med.* 34:159–182. http://dx.doi.org/10.1016/j.mam.2012.10.008

Russell, J.M., and W.F. Boron. 1976. Role of choloride transport in regulation of intracellular pH. *Nature.* 264:73–74. http://dx.doi.org/10.1038/264073a0

Silva, P., J. Stoff, M. Field, L. Fine, J.N. Forrest, and F.H. Epstein. 1977. Mechanism of active chloride secretion by shark rectal gland: role of Na-K-ATPase in chloride transport. *Am. J. Physiol.* 233:F298–F306.

Simpson, J.E., C.W. Schweinfest, G.E. Shull, L.R. Gawenis, N.M. Walker, K.T. Boyle, M. Soleimani, and L.L. Clarke. 2007. PAT-1 (Slc26a6) is the predominant apical membrane Cl^-/HCO_3^- exchanger in the upper villous epithelium of the murine duodenum. *Am. J. Physiol. Gastrointest. Liver Physiol.* 292:G1079–G1088. http://dx.doi.org/10.1152/ajpgi.00354.2006

Tsuganezawa, H., K. Kobayashi, M. Iyori, T. Araki, A. Koizumi, S. Watanabe, A. Kaneko, T. Fukao, T. Monkawa, T. Yoshida, et al. 2001. A new member of the HCO_3^- transporter superfamily is an apical anion exchanger of β-intercalated cells in the kidney. *J. Biol. Chem.* 276:8180–8189. http://dx.doi.org/10.1074/jbc.M004513200

Walker, N.M., M. Flagella, L.R. Gawenis, G.E. Shull, and L.L. Clarke. 2002. An alternate pathway of cAMP-stimulated Cl secretion across the NKCC1-null murine duodenum. *Gastroenterology.* 123:531–541. http://dx.doi.org/10.1053/gast.2002.34757

Wang, C.Z., H. Yano, K. Nagashima, and S. Seino. 2000. The Na^+-driven Cl^-/HCO_3^- exchanger. Cloning, tissue distribution, and functional characterization. *J. Biol. Chem.* 275:35486–35490. http://dx.doi.org/10.1074/jbc.C000456200

Wang, Z., L. Conforti, S. Petrovic, H. Amlal, C.E. Burnham, and M. Soleimani. 2001. Mouse Na^+: HCO_3^- cotransporter isoform NBC-3 (kNBC-3): cloning, expression, and renal distribution. *Kidney Int.* 59:1405–1414. http://dx.doi.org/10.1046/j.1523-1755.2001.0590041405.x

Zhang, G.H., E.J. Cragoe Jr., and J.E. Melvin. 1993. Na^+ influx is mediated by Na^+-K^+-$2Cl^-$ cotransport and Na^+-H^+ exchange in sublingual mucous acini. *Am. J. Physiol.* 264:C54–C62.

Zhang, W., D.G. Ogando, J.A. Bonanno, and A.G. Obukhov. 2015. Human SLC4A11 is a novel NH_3/H^+ co-transporter. *J. Biol. Chem.* 290:16894–16905. http://dx.doi.org/10.1074/jbc.M114.627455

Zhao, J., E.M. Hogan, M.O. Bevensee, and W.F. Boron. 1995. Out-of-equilibrium CO_2/HCO_3^- solutions and their use in characterizing a new K/HCO_3 cotransporter. *Nature.* 374:636–639. http://dx.doi.org/10.1038/374636a0